A Structural Model for Phosphorylation Control of *Dictyostelium* Myosin II Thick Filament Assembly

Wenchuan Liang, Hans M. Warrick, and James A. Spudich

Department of Biochemistry, Stanford University School of Medicine, Stanford, California 94305-5307

Abstract. Myosin II thick filament assembly in *Dictyostelium* is regulated by phosphorylation at three threonines in the tail region of the molecule. Converting these three threonines to aspartates (3×Asp myosin II), which mimics the phosphorylated state, inhibits filament assembly in vitro, and 3×Asp myosin II fails to rescue myosin II–null phenotypes. Here we report a suppressor screen of *Dictyostelium* myosin II–null cells containing 3×Asp myosin II, which reveals a 21-kD region in the tail that is critical for the phosphorylation control. These data, combined with new structural evidence from electron microscopy and sequence analyses, provide evidence that thick filament assembly control involves the folding of myosin II into a bent monomer, which is unable to incorporate into thick filaments. The data are consistent with a structural model for the bent monomer in which two specific regions of the tail interact to form an antiparallel tetrameric coiled–coil structure.

Key words: myosin II • thick filament assembly • *Dictyostelium* • phosphorylation • suppressor screen

THE spatial and temporal control of the assembly and disassembly of organelles is fundamental to cell and developmental biology. The cytoskeleton is particularly dynamic in vivo, responding to both internal and external signals that induce rapid changes in assembly state. A key component of the actin-based cytoskeleton is myosin II, which has been shown to be essential for cytokinesis of *Dictyostelium* cells in suspension as well as for efficient chemotaxis and morphogenetic changes in shape during development (De Lozanne and Spudich, 1987; Knecht and Loomis, 1987; Zang and Spudich, 1998). All of these roles require myosin II to be in the form of thick filaments.

A myosin II molecule consists of a pair of heavy chains and two pairs of light chains. Each heavy chain starts with an NH_2-terminal globular head, which has ATPase and motor activity, followed by a long α-helical tail. Analysis of the tail sequences of muscle and nonmuscle myosin IIs reveals multiple repeating patterns throughout the entire domain that enable the two tails to form an α-helical coiled–coil rod. The smallest repeat motif consists of seven amino acids occupied at position a–g in the helical turn. Generally, small and hydrophobic residues are found in positions a and d, which form the core and are essential to the formation of the coiled–coil structure (Parry, 1981). In all myosin IIs examined, the region of the coiled–coil tail that is required for assembly into thick filaments is in the COOH-terminal half of the tail.

In *Dictyostelium*, myosin II molecules constantly relocate to multiple locations for participating in various processes. When a cell migrates, myosin II accumulates in the posterior of the cell. During cell division, myosin II accumulates in the cleavage furrow. To accomplish its cellular tasks, myosin II is thought to assemble into bipolar thick filaments and pull together oppositely oriented actin filaments to produce contractile forces. Mutant forms of myosin II that do not assemble into bipolar thick filaments in vitro fail to rescue myosin-null phenotypes, and they do not localize to the furrow during cytokinesis (Fukui et al., 1990; Sabry et al., 1997). Interestingly, neither motor activity nor the existence of the myosin catalytic domain is necessary for myosin II transportation in cells (Yumura and Uyeda, 1997; Zang and Spudich, 1998).

The mechanism for *Dictyostelium* myosin filament assembly is thought to proceed in two distinctive stages. The initial slower step occurs by sequential association of myosin II monomers into parallel dimers and antiparallel tetramers. The next step is rapid lateral addition of myosin dimers to bipolar nuclei to form thick filaments (Mahajan and Pardee, 1996). A single point mutation in the tail domain has been shown to be sufficient to inhibit *Dictyostelium* myosin II filament assembly in vitro, apparently by preventing the formation of dimers and antiparallel tetramers (Moores and Spudich, 1998).

The initial step of filament assembly for *Dictyostelium* myosin II is thought to be induced by dephosphorylation

Address correspondence to James A. Spudich, Department of Biochemistry, Stanford University School of Medicine, Beckman Center, Stanford, CA 94305-5307. Tel.: (650) 723-7634. Fax: (650) 723-6783. E-mail: jspudich@cmgm.stanford.edu

of phosphorylated sites in the tail. Target sites for this phosphorylation control have been mapped to three threonines at positions 1823, 1833, and 2029 (denoted TTT) (Vaillancourt et al., 1988; Luck-Vielmetter et al., 1990). These three threonines are located in a regulatory domain that is ~23% (34 kD) of the length of the tail, starting from the COOH terminus. A short designation for myosins with different amino acids at positions 1823, 1833, and 2029 takes the form of XXX, where X uses the single amino acid code at each of the three positions. NH_2-terminal to the regulatory domain, another 34-kD region has been shown to be the smallest fragment of *Dictyostelium* myosin II that is necessary and sufficient for self-assembly (O'Halloran et al., 1990; Shoffner and De Lozanne, 1996). This region is denoted as the assembly domain.

Pasternak et al. (1989) reported evidence from electron microscopy that phosphorylation of the heavy chain promoted a bent conformation of myosin II at approximately two-thirds the length of the tail from the head-neck junction, and these bent myosin II molecules appeared to be excluded from the myosin filament. Further information was obtained from mutant myosin IIs, with the phosphorylatable threonines replaced by either three aspartates or three alanines, expressed in myosin II–null cells (denoted 3×Asp and 3×Ala cells, respectively) (Luck-Vielmetter et al., 1990; Egelhoff et al., 1993). 3×Asp myosin II mimicked the phosphorylated state, did not assemble into thick filaments in vitro, and failed to rescue myosin II–null phenotypes. Opposite to the 3×Asp mutant, 3×Ala myosin II assembled similar to wild-type myosin II in vitro. These data led to the hypothesis that after being phosphorylated, myosin II monomers prefer a bent conformation that is not able to assemble into parallel dimers, the initial unit for filament assembly (Pasternak et al., 1989). In this report we present a structural model for the myosin II bent monomer and provide evidence that two specific alanine-rich regions of the tail interact to form an antiparallel tetrameric coiled–coil structure.

Materials and Methods

Cell Culture

Dictyostelium myosin II–null cells (HS1), transformed with pBigMyD to create wild-type myosin II cells (Ruppel et al., 1994) and with pBIG-ASP to create 3×Asp myosin II cells, were grown as described (Egelhoff et al., 1993). The HL-5 growth medium was supplemented with 60 μg/ml streptomycin, 60 U/ml penicillin, and 5 μg/ml G418 (Geneticin; Life Technologies, Inc.). Bacterial lawns were prepared by spreading 2 ml of an overnight *Klebsiella aerogenes* culture on SM/5 plates (Sussman, 1987). Transformations were performed by electroporation (Egelhoff et al., 1991a) and transformed cells were selected by 5 μg/ml G418.

Mutagenesis and Clonal Isolation of Suppressors for 3×Asp Myosin II Cells

Suppressors of 3×Asp myosin II cells were generated by treatment with 4-nitroquinoline-*N*-oxide (NQNO)[1] or UV irradiation. Conditions for treatment of 3×Asp myosin II cells using chemical mutagen NQNO were as described by Patterson and Spudich (1995). After treatment with NQNO, cells were shaken in suspension for 30 min, washed twice with HL-5, and 1.2×10^6 cells were plated onto bacterial lawns. For suppressors generated by UV irradiation, 1.2×10^6 3×Asp myosin II cells were spotted onto plates containing bacterial lawn and irradiated with UV (0.8–6.4 mJ/cm^2).

Plates from either treatment were placed at 22°C and the developmental phenotype was observed 5 d later to screen for suppressors, which recovered the ability to sporulate. Clonal isolation of suppressors was performed as follows: a single sorus from each plaque was picked by a sterile pipet tip, resuspended in 5 ml HL-5, and spread on a new bacterial lawn to obtain single plaques.

Mutation Mapping and Reconstruction

The tail region of each suppressor was sequenced using standard methods to locate each mutation. The mutations were then introduced into the 3×Asp myosin II sequence by PCR overlap extension mutagenesis (Ho et al., 1989), and then subcloned into pLittleMyo (Moores and Spudich, 1998). These constructs were subsequently transformed into myosin II–null cells, and the developmental phenotypes were examined.

Electrophoresis and Immunoblotting

Whole-cell lysates were electrophoresed on SDS/7.5% polyacrylamide gels and transferred to nitrocellulose paper. The paper was probed with anti-*Dictyostelium* myosin II mAbs, My6 (Peltz et al., 1985) or mAb 55 (kindly provided by Dr. Guenther Gerisch, Max Planck Institut für Biochemie, Martinsried, Germany) (Pagh and Gerisch, 1986), and then incubated with a HRP-coupled secondary antibody (Bio-Rad). Signals were visualized with an enhanced chemiluminescence system (DuPont).

Protein Purification

Wild-type and 3×Asp myosin IIs were purified from cells grown and harvested as described (Egelhoff et al., 1993), after a modified purification protocol that does not require filament assembly (Moores and Spudich, 1998). After being washed with 10 mM Tris-HCl, 1 mM EDTA, pH 7.5, the cell pellets were resuspended in 2 vol/g cells 25 mM Hepes, 50 mM NaCl, 2 mM EDTA, 1 mM DTT, pH 7.4, containing a mixture of protease inhibitors (buffer A) (Moores and Spudich, 1998). The cell suspension was frozen by dripping into liquid nitrogen and stored at −80°C. Immediately before preparation, frozen pellets were thawed and lysed in 7 vol/g cells buffer A at 0°C. After sedimentation at 36,000 *g* for 30 min, the pellets were suspended in 4 vol/g cells 10 mM Hepes, 130 mM NaCl, 1 mM EDTA, 1 mM DTT, pH 7.4. The cell suspension was centrifuged at 36,000 *g* for 15 min. Extraction of myosin II was achieved by resuspending the pellets in 1.5 vol/g cells 10 mM Hepes, 150 mM NaCl, 5 mM $MgCl_2$, 4 mM ATP, and 1 mM DTT, pH 7.4. After centrifugation at 200,000 *g* for 30 min, RNase A (5 μg/ml) and PMSF (0.1 mM) were added to the supernatant. The solution was dialyzed against a 12% Aquacide III (Calbiochem) solution in 10 mM Hepes, 200 mM NaCl, 1 mM DTT, pH 7.4, to concentrate the volume ~20-fold, and further dialyzed in 10 mM Hepes, 200 mM NaCl, 1 mM DTT, pH 7.4 (column buffer). After adding 0.6 M potassium iodide, 20 mM sodium pyrophosphate, and 2 mM ATP, the concentrated dialysate was loaded onto a Biogel A15 gel (Bio-Rad) filtration column (80 ml total volume), which had been equilibrated previously with column buffer and preloaded with 10 ml 0.6 M KI, 20 mM NaPPi. Fractions containing myosin II were pooled and concentrated as mentioned before. Typical final concentrations for myosin IIs were 1–3 mg/ml, as determined by the Bradford method (Bradford, 1976), using rabbit skeletal muscle myosin II as the standard.

Rotary Shadowing EM and Analysis

Samples were diluted to 30–50 μg/ml myosin II in 50–70% glycerol, 10 mM Hepes, 200 mM KCl, 1 mM DTT, pH 7.4, and sprayed immediately onto freshly cleaved mica and viewed as described (Flicker et al., 1985). The locations of bends along the tail of myosin II monomers were measured on prints.

Results

Suppressors for 3×Asp Myosin II Cells Were All Intragenic

We used a random mutagenesis approach to identify suppressors responsible for recovery of myosin II function for

1. *Abbreviation used in this paper:* NQNO, 4-nitroquinoline-*N*-oxide.

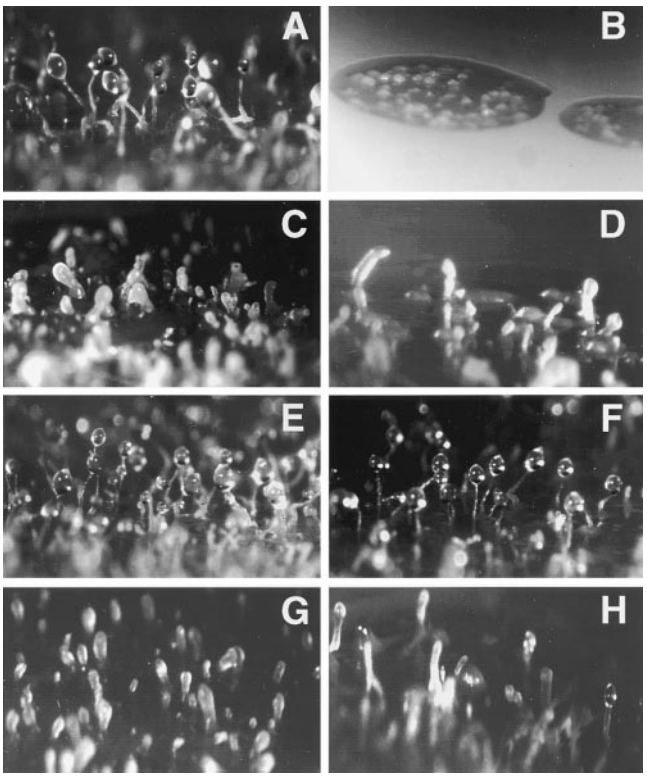

Figure 1. Developmental phenotypes of *Dictyostelium* cells expressing various forms of myosin II in the myosin II–null cells. (A) Wild-type myosin II. (B) 3×Asp myosin II. The developmental phenotype of 3×Asp myosin II cells is identical to that of the myosin II–null cells. (C) Myosin II from a limited suppressor. (D) Myosin II from a medium suppressor. (E) Myosin II from a full suppressor. (F) Recreated full suppressor mutant 3×Asp-D1823Y. (G) Recreated limited suppressor mutant 3×Asp-R1880P. (H) Recreated medium suppressor mutant 3×Asp-Δ1968.

3×Asp myosin II cells. 3×Asp myosin II cells are phenotypically identical to myosin II–null cells (Egelhoff et al., 1993). Both fail to complete the *Dictyostelium* developmental cycle. They arrest at the mound stage (Fig. 1 B). After treatment of cells with the chemical mutagen NQNO or UV irradiation, 3×Asp myosin II cells were spread on bacterial lawns. Any colony that developed past the mound stage was scored as a suppressor. Depending on the extent of suppression, the suppressors were sorted into three groups: limited, medium, and full (Fig. 1, C–E).

Mutagenesis was performed on a strain of *Dictyostelium* that had its endogenous *mhcA* gene deleted (HS1) and contains an extrachromosomal plasmid expressing *mhcA*–3×Asp myosin II (pBIG-ASP). To check whether the suppressor mutations were intragenic or extragenic, the plasmid from each suppressor was rescued and retransformed into unmutagenized myosin II–null cells, and the transformed cells were spread on bacterial lawns. The phenotypes of all the suppressors were reproduced, verifying that all 28 suppressor mutations were intragenic. The characteristics of the suppressors are shown in Table I. Typically the expression level of myosins from the suppressors was similar to that from the wild-type and 3×Asp myosin

Table I. Characteristics of Suppressors

Suppressor name	Method created	Extent of suppression*	No. of occurrences
Full-length myosin			
mhcA D1823Y	NQNO	Full	1
mhcA R1880P	NQNO	Limited	3
mhcA A1914P	NQNO	Limited	1
mhcA R1926P	NQNO	Limited	2
Truncated myosin			
mhcA Δ1968	UV	Medium	2
mhcA Δ1929–1930	NQNO	Medium	1
mhcA Δ1941–1945	UV	Limited	2
mhcA Δ1962–1967	UV	Limited	1
mhcA Δ1989–1995	NQNO, UV	Limited	2
mhcA Δ1999–2004	UV	Limited	1
mhcA Δ1987–2116	UV	Limited	1
mhcA Δ COOH terminus	NQNO, UV	Full, medium, limited	11

*Suppressors with full suppression have the phenotype identical to the wild-type. With limited suppression, suppressors display short stalks with no or opaque heads. Medium is between the full and limited suppression. See Fig. 1. Truncated myosin suppressors lacked the COOH terminus, but their sizes were the same or larger than ΔC34–myosin. See text.

II cells, but the size of the myosins varied (Fig. 2). 7 of 28 of the suppressors were full-length myosin II, 9 were small internal deletions of 1–7 residues, and 12 were truncations from the COOH terminus. There was no correlation between the means of mutagenesis (NQNO or UV) and the sizes of myosin IIs expressed from the suppressors. The sizes of the 12 ΔCOOH terminus suppressor myosin IIs were the same or larger than a previously studied mutant myosin II called ΔC34. ΔC34–myosin II, a truncated *Dictyostelium* myosin II lacking the 34-kD COOH terminus of the tail (the regulatory domain, residues 1819–2116; see Fig. 3), constitutively assembles into thick filaments, and ΔC34–myosin cells are able to complete the *Dictyostelium* developmental cycle and form fruiting bodies (O'Halloran and Spudich, 1990). Our ΔCOOH terminus myosin II suppressors are likely to be longer variants of the ΔC34–myosin II constitutive assembly phenotype, and we therefore focused on the remaining 16 suppressors.

The Myosin II Suppressor Mutations All Mapped to a Specific Region of the Tail

Sequencing results for all of the 16 full-length or near full-length suppressors revealed mutations that strikingly all lie in a 21-kD region (~182 amino acids) towards the COOH terminus of the tail (Fig. 3). All of the seven suppressors with single residue mutations resulted from changes of a single nucleotide base pair. The strongest suppressor was strain D1823Y, which had an aspartate to tyrosine mutation at position 1823 (denoted YDD). This position is one of the three targets for myosin II heavy chain kinase (Egelhoff et al., 1993). This residue corresponds to position d in the heptad repeat of the myosin II tail. The rest of the suppressors with single residue changes resulted in the introduction of a proline, which does not exist in the tail of wild-type *Dictyostelium* myosin II. Interestingly, three independent suppressors recovered from our screen affected Arg 1880, and two affected Arg

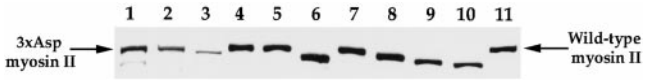

Figure 2. Examples of expression of myosin II from suppressors. Expression of mutant myosin IIs in the myosin II–null cell line HS1 transformed with the following suppressor mutants of 3×Asp myosin II: lane 1, 3×Asp myosin II control; lane 2, D1823Y; lane 3, ΔCOOH terminus1; lane 4, R1880P; lane 5, Δ1999–2004; lane 6, ΔCOOH terminus2; lane 7, R1880P; lane 8, ΔCOOH terminus3; lane 9, ΔCOOH terminus4; lane 10, ΔCOOH terminus5; and lane 11, wild-type myosin II control. The ΔCOOH terminus suppressors were revealed by immunoblotting experiments using the mAb 55, which binds an epitope at the COOH terminus of the tail (Pagh and Gerisch, 1986). They failed to bind mAb 55.

1926. Such multiple hits imply that these positions may play critical roles in regulating filament assembly. The nine small internal deletion group of suppressors had deletions of one to seven amino acids in this region. As shown in Fig. 3 B, the locations of the deletion and the single-residue mutation groups did not mix. The deletions all mapped beyond position 1926.

To be certain that the mapped mutations were responsible for the suppression phenotype and not mutations elsewhere in the myosin II that we may have missed, these mutations were recreated using PCR overlap extension mutagenesis of a 3×Asp myosin II gene contained within an extrachromosomal *Dictyostelium* expression vector. The plasmids were transformed into myosin II–null cells and the development ability on bacterial lawns was tested. The sporulation phenotypes were identical to the original suppressor strains (e.g., see Fig. 1, F–H).

Electron Microscopy Reveals that 3×Asp Myosin II Is Mainly in a Bent Monomer Conformation

Dictyostelium 3×Asp myosin II molecules were monomeric at high ionic strength. Rotary shadowed 3×Asp myosin II exhibited primarily two conformations under this condition: straight and bent monomers (Fig. 4 A). Various forms of the bent monomers were observed. In 20% of the bent monomer images, the COOH terminus of the tail folded back tightly and resulted in an apparently shorter tail (Fig. 4 A, lower panel). 77% of the 3×Asp myosin II molecules were found to be in the bent conformation (n = 400). On the other hand, only 23% of the wild-type myosin II molecules were found to be bent (n = 280). The percentage of the bent wild-type molecules is consistent with the previous finding that freshly purified wild-type myosin IIs are 20–30% phosphorylated in the heavy chain (Kuczmarski and Spudich, 1980).

The majority of the 3×Asp myosin II molecules bend at ~1,200 Å, located at approximately two-thirds the length of the tail from the head–neck junction (Fig. 4 B). This bent position is similar to that measured for wild-type myosin II monomers (Pasternak et al., 1989). However, we also observed a previously unfound, minor population of bends at ~1,000 Å (Fig. 4 B). These values are interesting, in that they fit well with the structural motifs described below for the myosin II tail. The relative proportion of bends at 1,000 and 1,200 Å appeared to be the same in 3×Asp and wild-type myosins (~35%).

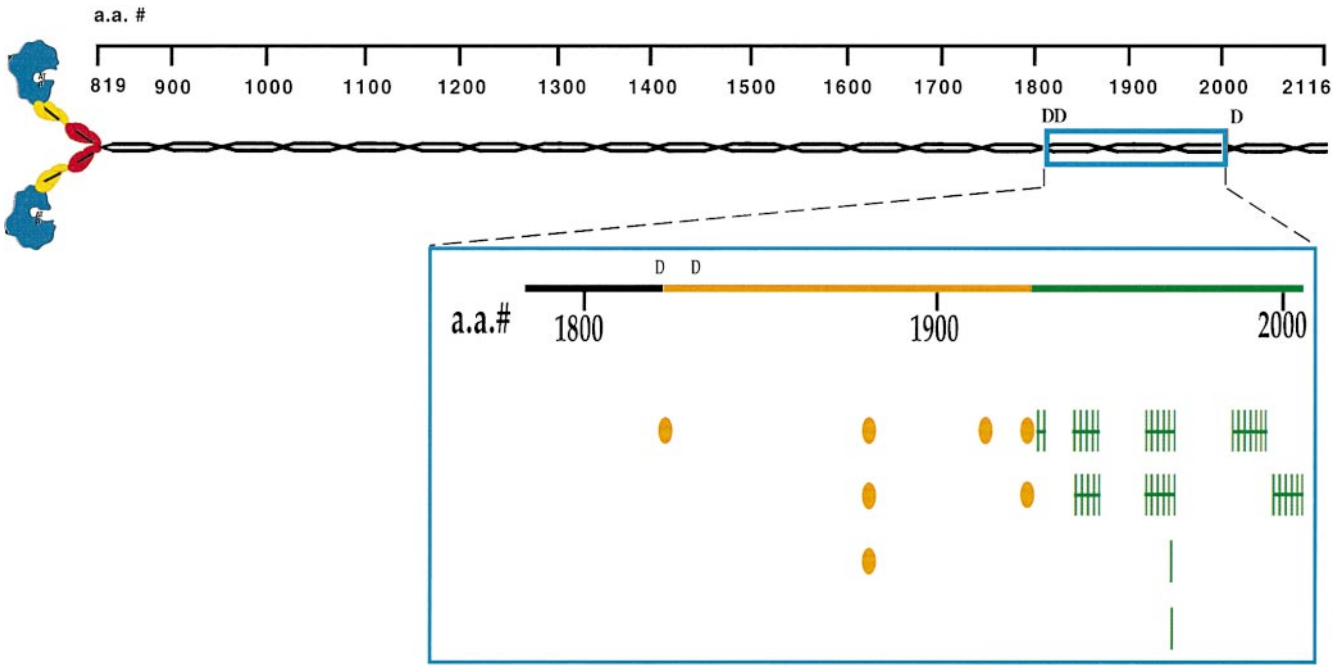

Figure 3. Mapping of myosin II mutations from suppressors. Diagrammatic representation of the mutations in the *Dictyostelium* myosin II molecule. All of the mutations were packed into a window of 182 amino acids shown in the box. Suppressors with single residue were displayed by orange dots. Suppressors with deletion mutations were displayed by green bar(s). One vertical bar represents deletion of one amino acid. The orange line denotes a region containing only point mutations and the green line indicates a region containing only deletion mutations.

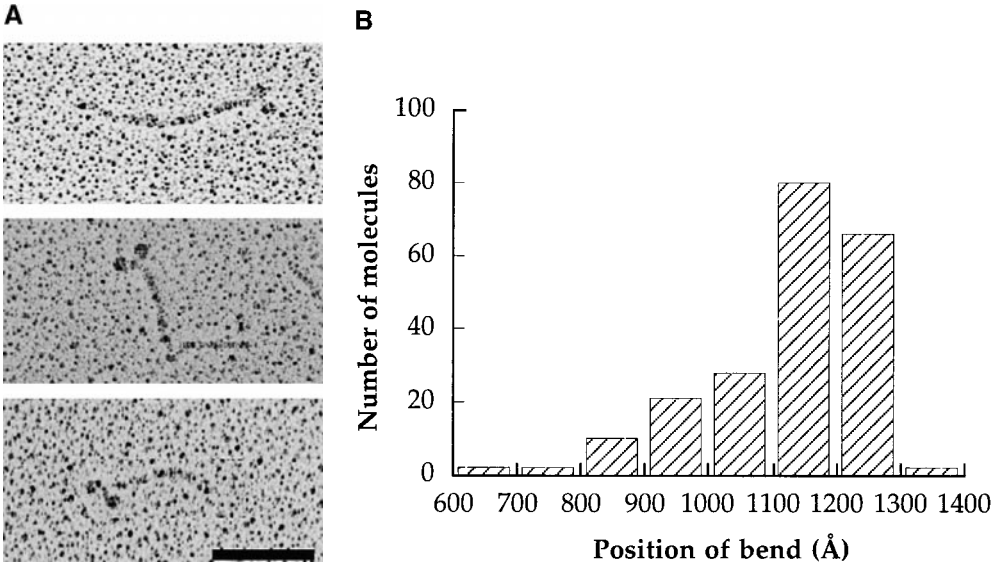

Figure 4. Representative rotary shadowed myosin II molecules in high ionic strength (200 mM KCl). (A) Upper panel: myosin II molecule in the straight conformation. Middle panel: myosin II molecule in a bent conformation. Lower panel: an extreme case of the bent conformation, where the COOH terminus of the tail folds back tightly to make the molecule look shorter. Bar, 0.1 μm. (B) Position of bend in EM images of 3×Asp myosin II monomers. The majority of 3×Asp myosin IIs bend at 1,200 Å, approximately two-thirds length of the tail from the head–neck junction. A second region at ~1000 Å was also observed. $n = 210$.

The tail domain of *Dictyostelium* myosin II consists of 1,298 residues, and has no proline interruptions. The coiled–coil prediction algorithm Coils (Lupas et al., 1991) predicts small, distinct regions in the *Dictyostelium* myosin II tail that have low probabilities to form a coiled–coil structure (Fig. 5). The two most unfavorable regions for coiled–coil structure locate at ~1,000 and 1,200 Å from the head–neck junction. Consistent with this prediction, to optimize the pattern of charged and uncharged residues for the periodicity of stable coiled–coil structure in the tail, two skips of two amino acids each were necessary to be inserted into the tail sequence lineup at these two regions (Warrick et al., 1986). Similar correlation between the bends observed from EM versus skips in the tail has been shown in smooth and skeletal muscle myosins (Offer, 1990), and in *Acanthamoeba* myosin (Hammer et al., 1987). These results indicate that these two positions at ~1,000 and 1,200 Å from the head–neck junction are hinge regions in the *Dictyostelium* tail domain, as seen in other myosin IIs (Tan et al., 1992).

In another region of the tail, closer to the myosin head (~400 Å from the head–neck junction), there is a small area that has a somewhat lower probability to be in a coiled–coil than the majority of the tail (Fig. 5). In *C. elegans*, a similar domain has been described as the prehinge (Hoppe and Waterston, 1996). A similar region (~440 Å from the head–neck junction) predicted from muscle myosin IIs has been proposed to serve as a hinge, which allows the head domain to swing away from the thick filament, thus allowing the myosin heads greater freedom to interact with the actin filaments (Offer, 1990).

Alanine-rich Core Domains in the Tail Are Consistent with an Antiparallel Tetrameric Coiled–Coil Structure

An analysis of the *Dictyostelium* myosin II tail sequence revealed two regions (denoted A and B) in the tail that are unusually rich in alanine residues at the core (a or d) positions of the heptad repeats (Fig. 6). Region A spans 18 heptad repeats (between residue numbers 1383 and 1508). Region B contains 23 heptad repeats (residue 1806–1966). More than 75% of all of the alanines at core a and d positions along the tail are found in regions A and B, although these regions account for only 22% of the total tail. The 300–amino acid gap between regions A and B contains the previously identified assembly domain (O'Halloran et al., 1990), which contains only two alanines. The midpoint of the gap is at ~1,200 Å from the head–neck junction. Core a and d positions rich in alanine residues have been shown to be important for the proper packing of four α-helices into an antiparallel α-helical coiled–coil structure (Monera

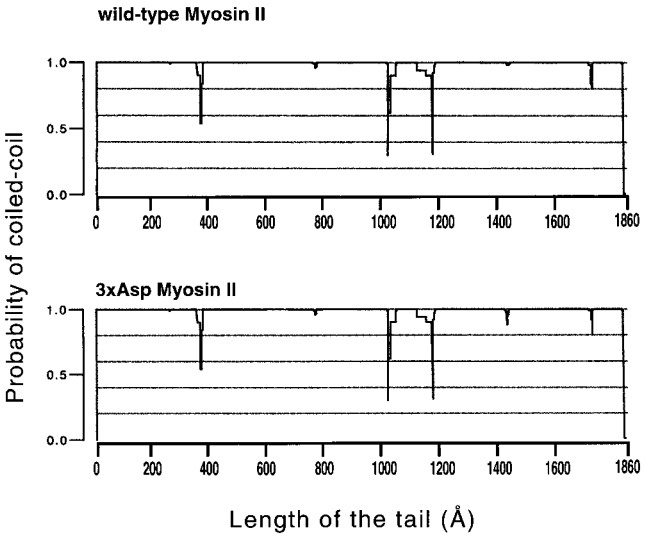

Figure 5. Coiled–coil predictions of *Dictyostelium* wild-type and 3×Asp myosin IIs. The predictions were generated by the Coils program (Lupas et al., 1991). x-axis, amino acid positions starting from the head–neck junction. y-axis, probability of forming a coiled–coil. A window of 28 amino acids was used to generate the profiles shown.

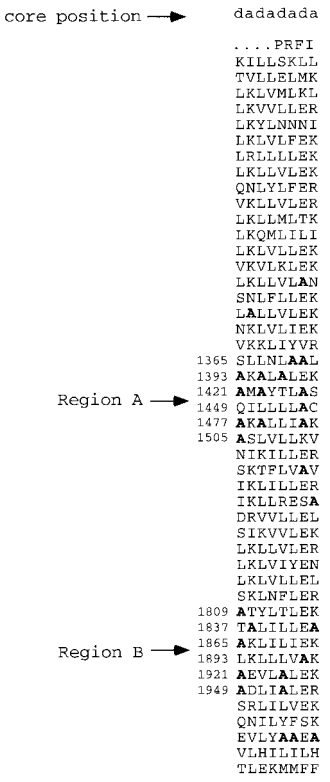

Figure 6. Alanine-rich domains in the tail of *Dictyostelium* myosin II. The core a and d positions are shown for the entire myosin II tail. Regions A and B are unusually rich in alanine residues (shown in bold) at the core positions of the coiled–coil structure. The number of the first residue in each row in these two regions is shown.

et al., 1996). Moreover, X-ray crystal structure determination indicates that the ColE1 Rop protein forms a highly regular four stranded α-helix bundle with alanine residues populated in the hydrophobic core (Banner et al., 1987).

Discussion

The results presented here, together with earlier results (Pasternak et al., 1989; Tan et al., 1992), suggest the following structural model of phosphorylation control of myosin II thick filament assembly (Fig. 7). Phosphorylation by myosin II heavy chain kinase produces charges on the outside of the coiled–coil tail that help stabilize the bent form of the myosin. Bent myosin II molecules cannot associate with other molecules to form parallel dimers, and therefore no antiparallel tetramers appear for the next phase of filament formation. Myosin II heavy chain phosphatase removes phosphates from the bent monomers, and the molecules return to their straight conformation. We propose that the threonine pair 1823/1833 could act as a nucleation site, which when phosphorylated, initiates the bent monomer conformation by orienting the two strands of dimeric coiled–coils. Once nucleated, regions A and B may zip up into an antiparallel four-stranded structure, possibly similar to that observed for the ColE1 Rop protein (Banner et al., 1987). Formation of such a structure results in a major bend at ~1,200 Å from the head–neck junction. Moreover, the previously identified assembly domain (Fig. 7, blue) (O'Halloran and Spudich, 1990) is sequestered as a loop between regions A and B. This conformation of the assembly domain prevents intermolecular interactions that lead to formation of thick filaments. The equilibrium between the bent versus straight conformations is delicately poised, and can be easily disturbed by mutations at multiple sites in the tail (e.g., the suppressor mutations described here; see also Moores and Spudich, 1998).

Position 1823 appears to be a particularly critical position for switching between the bent and open conformations. YDD is the only suppressor with a full-length myosin II that completely restores wild-type development. With the aspartate to tyrosine mutation at position 1823, YDD revives myosin II functions possibly by removing the negatively charged aspartate at position 1823 in 3×Asp myosin II that participates in an electrostatic interaction needed for the formation of the bent monomer. Unlike the other two myosin heavy chain kinase sites, residue 1823 corresponds to position d of the heptad repeat of the myosin tail. Position d is at the core of the coiled–coil, which most commonly consists of hydrophobic residues. To tolerate a negatively charged residue at this position in the bent conformation, it is conceivable that a positively charged residue(s) from region A contributes in the core of the antiparallel tetrameric coiled–coil structure. Two possible candidates are lysine 1481 or 1526, at positions a and d, respectively. An interruption of the heptad repeat by polar residues has been observed in the SNARE complex, which is also a highly regulated tetrameric coiled–coil structure (Sutton et al., 1998).

The relative importance of the three threonine targets for myosin heavy chain kinase and phosphatase have been explored by constructing all possible combinations of threonines and aspartates and examining the myosin II functions (Nock, S., W. Liang, H. Warrick, and J.A. Spudich, unpublished data). Consistent with the current report, threonine 1823 appears to be the most critical phosphorylation site for myosin II functions. Simply replacing aspartate at position 1823 with a threonine in 3×Asp myosin II (denoted TDD) is enough to reverse the null phenotypes into wild-type. On the other hand, DTD partially recovers myosin II function, which indicates that position 1833 does play some role. Position 2029 does not appear to be required, because DDT is identical to myosin-null cells. These arguments assume, of course, that an aspartate fully mimics a phosphorylated threonine.

Because TDD has a wild-type phenotype, it is interesting that we did not get a simple reversion from aspartate to threonine in our suppressor screen. This could be due to the fact that this mutation would require two nucleotide changes, which is expected to occur in lower probability. It has been reported that kinases that specifically phosphorylate the three threonines also accept serines (Luck-Vielmetter et al., 1990). The mutation from an aspartate to a serine would also require two nucleotide changes.

The interaction within the alanine-rich core regions A and B appears to be highly sensitive to even single amino acid changes in the tail. All of the suppressors with single point mutations other than YDD, are located in region B, and except for YDD, they all involve the replacement of an amino acid residue with proline. That a single proline at any of three positions appears to be sufficient to destabilize the antiparallel tetrameric coiled–coil domain is possibly explained by its well-known disruptive effect on α-helical structure. The locations of suppressors with proline substitutions (Fig. 7, orange) and deletion mutations (Fig.

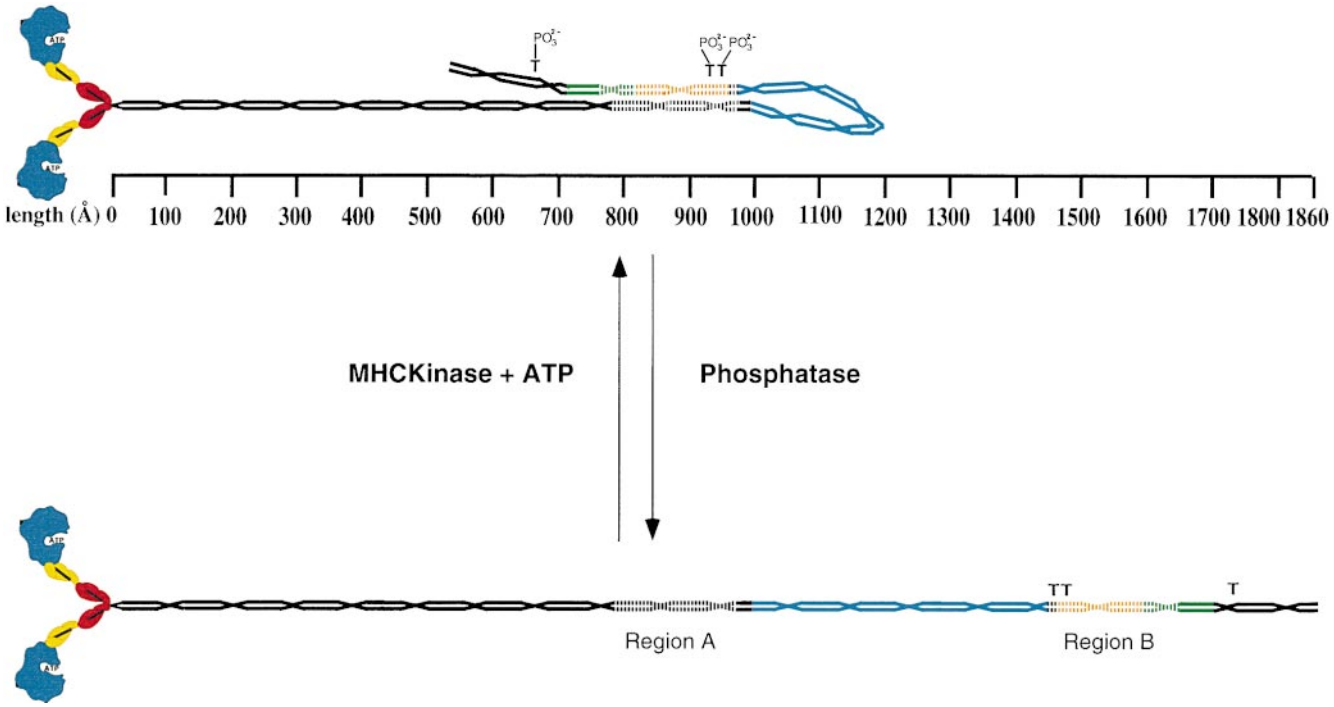

Figure 7. A model for the bent conformation responsible for the regulation of the initial step of filament assembly. We propose that regulation of the initial step of filament assembly results from the state of phosphorylation in the myosin II molecules. An unphosphorylated myosin II molecule in the straight conformation is shown below. The two regions (A and B) rich in alanines are shown in dashed patterns. Mutations mapped from the suppressors against 3×Asp myosins are shown in orange (for single point mutations) and green (for deletion mutations), and locate in region B. A bent phosphorylated myosin II molecule that folds at ~1,200 Å from the head–neck junction is shown, where the alanine-rich regions A and B overlap. Threonine pair 1823/1833 may be a nucleation site where the bent monomer conformation is initiated after phosphorylation, followed by the formation of an antiparallel tetrameric coiled–coil in the alanine-rich regions. The assembly domain (O'Halloran et al., 1990; Shoffner and De Lozanne, 1996; shown in blue) is sequestered as a looped structure that is unable to self-assemble into higher-order structures.

7, green) are distinctly clustered. This suggests that the interactions that lead to suppression are different in the two sections of domain B. In one section, prolines may destabilize the bent monomer by disrupting the tetrameric coiled–coil structure. In the other section, deletions may shift the alignment of the coiled–coil regions in the bent monomer, resulting in disruption of critical contacts such as salt bridges important for maintaining the bent monomer. It is important to note that the model described in Fig. 7 only deals with the first step of filament assembly. It is possible that the interactions identified by the suppressors could be between different molecules in higher ordered structures. These structures would be the subsequent steps of the filament assembly pathway. Thus, the proline mutations may locally disrupt the thick filament substructure such that the aspartate residues could be better accommodated. This could shift the equilibrium to favor filament formation. Similarly, the shift of alignment by the deletion mutations could disrupt critical contacts important for the thick filament structure.

It is interesting that no suppressors were found in region A. One possibility is that any mutation in this region affects another step in the pathway for thick filament assembly, which is therefore unable to survive our screening process. In fact, the second half of region A has been strongly implicated in formation of parallel dimers (Pasternak et al., 1989), which are the building blocks for thick filaments.

Several myosin II tail mutants have been constructed with COOH-terminal and internal deletions. COOH-terminal deletion mutants are functional to different extents as long as the assembly domain (Fig. 7, blue) is intact, allowing filaments to form (Egelhoff et al., 1991b; Lee et al., 1994). Mutants that remove parts of the proposed tetrameric coiled–coil structure (region B; Fig. 7, green and orange stripes) give rise to intermediate in vivo phenotypes, indicating that regulation is impaired (Lee et al., 1994). Deletions that remove fragments between the head and region A (Fig. 7, gray stripes) appear to be functional, but if part of region A is removed an intermediate phenotype is observed (Kubalak et al., 1992; Shu et al., 1999). These observations are consistent with the proposal that the tetrameric coiled–coil structure is important for efficient regulation.

Phosphorylation of myosin II heavy chain has been found to occur in a variety of nonmuscle cells as well as in the catch muscle of mollusks, and may be a general mechanism of regulating myosin II function (Tan et al., 1992). It is possible that the hinges in the tail domains of these other myosins are designed for regulation of myosin IIs through a mechanism similar to that proposed here. The

bending position of *Acanthamoeba* myosin II locates at a proportionally similar position as the *Dictyostelium* region (Hammer et al., 1987). Furthermore, the *Acanthamoeba* myosin II is phosphorylated at three serines located at the end of the tail (Collins et al., 1982). However, it is controversial whether phosphorylation regulates assembly of the *Acanthamoeba* myosin II (Collins et al., 1982; Sinard and Pollard, 1989).

Myosin II from a molluscan catch muscle is phosphorylated at two serines in the tail domain (Castellani et al., 1988). After phosphorylation, myosin II solubility is enhanced and the molecule folds (Castellani and Cohen, 1987), reminiscent of the behavior of *Dictyostelium* myosin II. Recently, heavy chain phosphorylation of vertebrate nonmuscle myosin IIs and even of smooth muscle myosin II has been reported (Korn and Hammer, 1988; Kelley and Adelstein, 1990; Fukui and Morita, 1996). It remains to be determined whether the model proposed in this study is universal to myosin IIs that are regulated by heavy chain phosphorylation.

Smooth muscle myosin II has two hinge regions located at approximately one-third and two-thirds the length of the tail from the head–neck junction domain (Tan et al., 1992). Although little is known regarding the effects of heavy chain phosphorylation for smooth muscle myosin, in vitro regulation of conformational changes in this myosin, and control of assembly has been reported to be mainly by light chain phosphorylation (Craig et al., 1983; Trybus, 1989). However, there is controversy about the state or the extent of light chain phosphorylation change in the filamentous state of smooth muscle myosin II in vivo (Post et al., 1995; Somlyo et al., 1981).

Cells have evolved intricate mechanisms for the control of macromolecular assemblies. The myosin II thick filament is just one example where a delicately balanced equilibrium between monomer and filament forms is used to control cellular function. The model suggested here proposes that phosphorylation on a single threonine residue on a >200-kD protein results in stabilization of a bent monomer form of the molecule. This structural modification shifts the equilibrium to make filament assembly less favorable. Specific kinases and phosphatases can be activated, repressed, or spatially distributed to provide the appropriate regulation signals. A related model has been proposed for the regulation of the activity of heat shock factor in *Drosophilia* (Rabindran et al., 1993). There, coiled–coil regions of the protein interact within the protein as a monomer or between proteins as the active trimer form. The regulation of macromolecular assemblies via coiled–coil interactions is likely a widely applicable, highly dynamic, important cellular mechanism.

We are grateful to Dr. Guenther Gerisch for his generous gift of the monoclonal antibody mAb 55. We thank Lynne Mercer for help with the electron microscopy and taking the electron microscopy pictures.

W. Liang is supported by a fellowship from the American Cancer Society. This work was supported by National Institutes of Health grant 46551 to J.A. Spudich.

Submitted: 29 July 1999
Revised: 30 September 1999
Accepted: 18 October 1999

References

Banner, D.W., M. Kokkinidis, and D. Tsernoglou. 1987. Structure of the ColE1 Rop protein at 1.7 Å resolution. *J. Mol. Biol.* 196:657–675.

Bradford, M.M. 1976. A rapid and sensitive method for the quantitation of microgram quantities of protein utilizing the principle of protein-dye binding. *Anal. Biochem.* 72:248–254.

Castellani, L., and C. Cohen. 1987. Rod phosphorylation favors folding in a catch muscle myosin. *Proc. Natl. Acad. Sci. USA.* 84:4058–4062.

Castellani, L., B.W.J. Elliott, and C. Cohen. 1988. Phosphorylatable serine residues are located in a non-helical tailpiece of a catch muscle myosin. *J. Muscle Res. Cell Motil.* 9:533–540.

Collins, J.H., G.P. Cote, and E.D. Korn. 1982. Localization of the three phosphorylation sites on each heavy chain of *Acanthamoeba* myosin II to a segment at the end of the tail. *J. Biol. Chem.* 257:4529–4534.

Craig, R., R. Smith, and J. Kendrick-Jones. 1983. Light-chain phosphorylation controls the conformation of vertebrate non-muscle and smooth muscle myosin molecules. *Nature.* 302:436–439.

De Lozanne, A., and J.A. Spudich. 1987. Disruption of the *Dictyostelium* myosin heavy chain gene by homologous recombination. *Science.* 236:1086–1091.

Egelhoff, T.T., S.S. Brown, and J.A. Spudich. 1991a. Spatial and temporal control of nonmuscle myosin localization: identification of a domain that is necessary for myosin filament disassembly in vivo. *J. Cell Biol.* 112:677–688.

Egelhoff, T.T., M.A. Titus, D.J. Manstein, K.M. Ruppel, and J.A. Spudich. 1991b. Molecular genetic tools for study of the cytoskeleton in *Dictyostelium*. *Methods Enzymol.* 196:319–334.

Egelhoff, T.T., R.J. Lee, and J.A. Spudich. 1993. *Dictyostelium* myosin heavy chain phosphorylation sites regulate myosin filament assembly and localization in vivo. *Cell.* 75:363–371.

Flicker, P.F., G. Peltz, M.P. Sheetz, P. Parham, and J.A. Spudich. 1985. Site-specific inhibition of myosin-mediated motility in vitro by monoclonal antibodies. *J. Cell Biol.* 100:1024–1030.

Fukui, Y., and F. Morita. 1996. Two phosphorylations specific to the tail region of the 204-kDa heavy chain isoform of porcine aorta smooth muscle myosin. *J. Biochem. (Tokyo).* 119:783–790.

Fukui, Y., A. De Lozanne, and J.A. Spudich. 1990. Structure and function of the cytoskeleton of a *Dictyostelium* myosin-defective mutant. *J. Cell Biol.* 110:367–378.

Hammer, J.A., III, B. Bowers, B.M. Paterson, and E.D. Korn. 1987. Complete nucleotide sequence and deduced polypeptide sequence of a nonmuscle myosin heavy chain gene from *Acanthamoeba*: evidence of a hinge in the rod-like tail. *J. Cell. Biol.* 105:913–925.

Ho, S.N., H.D. Hunt, R.M. Horton, J.K. Pullen, and L.R. Pease. 1989. Site-directed mutagenesis by overlap extension using the polymerase chain reaction. *Gene.* 77:51–59.

Hoppe, P.E., and R.H. Waterston. 1996. Hydrophobicity variations along the surface of the coiled–coil rod may mediate striated muscle myosin assembly in *Caenorhabditis elegans*. *J. Cell Biol.* 135:371–382.

Kelley, C.A., and R.S. Adelstein. 1990. The 204-kDa smooth muscle myosin heavy chain is phosphorylated in intact cells by casein kinase II on a serine near the carboxyl terminus. *J. Biol. Chem.* 265:17876–17882.

Knecht, D.A., and W.F. Loomis. 1987. Antisense RNA inactivation of myosin heavy chain gene expression in *Dictyostelium discoideum*. *Science.* 236:1081–1086.

Korn, E.D., and J.A. Hammer III. 1988. Myosins of nonmuscle cells. *Ann. Rev. Biophys. Biophys. Chem.* 17:23–45.

Kubalak, E.W., T.P.Q. Uyeda, and J.A. Spudich. 1992. A *Dictyostelium* myosin II lacking a proximal 58-kDa portion of the tail is functional in vitro and in vivo. *Mol. Biol. Cell.* 3:1455–1462.

Kuczmarski, E.R., and J.A. Spudich. 1980. Regulation of myosin self-assembly: phosphorylation of *Dictyostelium* heavy chain inhibits formation of thick filaments. *Proc. Natl. Acad. Sci. USA.* 77:7292–7296.

Lee, R.J., T.T. Egelhoff, and J.A. Spudich. 1994. Molecular genetic truncation analysis of filament assembly and phosphorylation domains of *Dictyostelium* myosin heavy chain. *J. Cell Sci.* 107:2875–2886.

Luck-Vielmetter, D., M. Schleicher, B. Grabatin, J. Wippler, and G. Gerisch. 1990. Replacement of threonine residues by serine and alanine in a phosphorylatable heavy chain fragment of *Dictyostelium* myosin II. *FEBS Lett.* 269:239–243.

Lupas, A., M. Van Dyke, and J. Stock. 1991. Predicting coiled coils from protein sequences. *Science.* 252:1162–1164.

Mahajan, R.K., and J.D. Pardee. 1996. Assembly mechanism of *Dictyostelium* myosin II: regulation by K^+, Mg^{2+}, and actin filaments. *Biochemistry.* 35: 15504–15514.

Monera, O.D., N.E. Zhou, P. Lavigne, C.M. Kay, and R.S. Hodges. 1996. Formation of parallel and antiparallel coiled-coils controlled by the relative positions of alanine residues in the hydrophobic core. *J. Biol. Chem.* 271:3995–4001.

Moores, S.L., and J.A. Spudich. 1998. Conditional loss-of-myosin-II-function mutants reveal a position in the tail that is critical for filament nucleation. *Mol. Cell.* 1:1043–1050.

Offer, G. 1990. Skip residues correlate with bends in the myosin tail. *J. Mol. Biol.* 216:213–218.

O'Halloran, T.J., and J.A. Spudich. 1990. Genetically engineered truncated myosin in *Dictyostelium*: the carboxyl-terminal regulatory domain is not re-

quired for the developmental cycle. *Proc. Natl. Acad. Sci. USA*. 87:8110–8114.

O'Halloran, T.J., S. Ravid, and J.A. Spudich. 1990. Expression of *Dictyostelium* myosin tail segments in *Escherichia coli*: domains required for assembly and phosphorylation. *J. Cell Biol.* 110:63–70.

Pagh, K., and G. Gerisch. 1986. Monoclonal antibodies binding to the tail of *Dictyostelium* discoideum myosin: their effects on antiparallel and parallel assembly and actin-activated ATPase activity. *J. Cell Biol.* 103:1527–1538.

Parry, D.A.D. 1981. Structure of rabbit skeletal myosin. Analysis of the amino acid sequences of two fragments from the rod region. *J. Mol. Biol.* 153:459–464.

Pasternak, C., P.F. Flicker, S. Ravid, and J.A. Spudich. 1989. Intermolecular versus intramolecular interactions of *Dictyostelium* myosin: possible regulation by heavy chain phosphorylation. *J. Cell Biol.* 109:203–210.

Patterson, B., and J.A. Spudich. 1995. A novel positive selection for identifying cold-sensitive myosin II mutants in *Dictyostelium*. *Genetics.* 140:505–515.

Peltz, G., J.A. Spudich, and P. Parham. 1985. Monoclonal antibodies against seven sites on the head and tail of *Dictyostelium* myosin. *J. Cell Biol.* 100: 1016–1023.

Post, P.L., R.L. DeBiasio, and D.L. Taylor. 1995. A fluorescent protein biosensor of myosin II regulatory light chain phosphorylation reports a gradient of phosphorylated myosin II in migrating cells. *Mol. Biol. Cell.* 6:1755–1768.

Rabindran, S.K., R.I. Haroun, J. Clos, J. Wisniewski, and C. Wu. 1993. Regulation of heat shock factor trimer formation: role of a conserved leucine zipper. *Science.* 259:230–234.

Ruppel, K.M., T.Q. Uyeda, and J.A. Spudich. 1994. Role of highly conserved lysine 130 of myosin motor domain. In vivo and in vitro characterization of site specifically mutated myosin. *J. Biol. Chem*. 269:18773–18780.

Sabry, J.H., S.L. Moores, S. Ryan, J.-H. Zang, and J.A. Spudich. 1997. Myosin heavy chain phosphorylation sites regulate myosin localization during cytokinesis in live cells. *Mol. Biol. Cell.* 8:2605–2615.

Shoffner, J.D., and A. De Lozanne. 1996. Sequences in the myosin II tail required for self-association. *Biochem. Biophys. Res. Commun.* 218:860–864.

Shu, S., R.J. Lee, J.M. LeBlanc-Straceski, and T.Q.P. Uyeda. 1999. Role of myosin II tail sequences in its function and localization at the cleavage furrow in *Dictyostelium*. *J. Cell Sci.* 112:2195–2201.

Sinard, J.H., and T.D. Pollard. 1989. The effect of heavy chain phosphorylation and solution conditions on the assembly of *Acanthamoeba* myosin-II. *J. Cell Biol.* 109:1529–1535.

Somlyo, A.V., T.M. Butler, M. Bond, and A.P. Somlyo. 1981. Myosin filaments have non-phosphorylated light chains in relaxed smooth muscle. *Nature.* 294:567–569.

Sussman, M. 1987. Cultivation and synchronous morphogenesis of *Dictyostelium* under controlled experimental conditions. *Methods Cell Biol.* 28:9–29.

Sutton, R.B., D. Fasshauer, R. Jahn, and A.T. Brunger. 1998. Crystal structure of a SNARE complex involved in synaptic exocytosis at 2.4 Å resolution. *Nature.* 395:347–353.

Tan, J.L., S. Ravid, and J.A. Spudich. 1992. Control of nonmuscle myosins by phosphorylation. *Ann. Rev. Biochem*. 61:721–759.

Trybus, K.M. 1989. Filamentous smooth muscle myosin is regulated by phosphorylation. *J. Cell Biol.* 109:2887–2894.

Vaillancourt, J.P., C. Lyons, and G.P. Cote. 1988. Identification of two phosphorylated threonines in the tail region of *Dictyostelium* myosin II. *J. Biol. Chem*. 263:10082–10087.

Warrick, H.M., A. De Lozanne, L.A. Leinwand, and J.A. Spudich. 1986. Conserved protein domains in a myosin heavy chain gene from *Dictyostelium discoideum*. *Proc. Natl. Acad. Sci. USA*. 83:9433–9437.

Yumura, S., and T.Q. Uyeda. 1997. Transport of myosin II to the equatorial region without its own motor activity in mitotic *Dictyostelium* cells. *Mol. Biol. Cell.* 8:2089–2099.

Zang, J., and J.A. Spudich. 1998. Myosin II localization during cytokinesis occurs by a mechanism that does not require its motor domain. *Proc. Natl. Acad. Sci. USA*. 95:13652–13657.